Progress in Nuclear Energy 175 (2024) 105332

Contents lists available at ScienceDirect

Progress in Nuclear Energy

journal homepage: www.elsevier.com/locate/pnucene

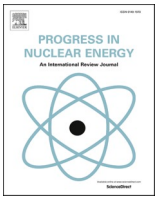

A novel automated thickness measurement method and device for nuclear fuel plates

Marcelo Kobayoshi [a], Ricardo Mendes Leal Neto [a], Elita Fontenele Urano de Carvalho [a], Thomaz Augusto Guisard Restivo [b], Michelangelo Durazzo [a,*]

[a] Nuclear and Energy Research Institute, IPEN-CNEN/SP, São Paulo, SP, Brazil
[b] University of Sorocaba, UNISO, Sorocaba, SP, Brazil

ARTICLE INFO

Keywords:
Fuel plate
Automated measurement
Metrological reliability
Measurement uncertainty
Nuclear fuel

ABSTRACT

The Nuclear and Energy Research Institute (IPEN-CNEN/SP) currently employs manual external u-shape frame micrometers with non-rotating spindles, and chamfered measuring anvils at 21 pre-defined points to control the thickness of its fuel plates. However, it is acknowledged that this method introduces the human element into the measurement process, potentially compromising result accuracy and the integrity of the fuel plates' surfaces. This research introduces a novel thickness measurement method and an accompanying automated device featuring precise movement mechanisms, data capture, transcription, and processing. Our findings emphasize the effectiveness of this new measurement system and the structural integrity of the equipment, highlighting its potential to significantly enhance both the speed and metrological reliability of dimensional control processes for nuclear fuel plates manufactured at IPEN-CNEN/SP.

1. Introduction

The fuel elements manufactured at IPEN-CNEN/SP (Nuclear and Energy Research Institute) are of the MTR (Materials Testing Reactor) type (Cunningham and Boyle, 1955). They are built by assembling a number of fuel plates with sufficient spacing between them to allow the flow of water, which serves as both coolant and moderator. As shown in Fig. 1, the MTR-type fuel is composed of an array of parallel fuel plates that are rigidly put together to form the fuel element. The fuel plates are formed by a "meat" containing the fissile material, which is entirely protected with an aluminum cladding (Weber and Hirsch, 1955). The fuel plates are manufactured using a traditional method, known internationally as the "picture frame technique", shown in Fig. 2 (Durazzo and Riella, 2015; Kaufman, 1962). This involves inserting the fuel meat (also called "briquette") into an aluminum frame and covering it with aluminum plates that are then rolled together.

The various structures comprising the fuel element must maintain their shape and integrity over extended periods of use, ensuring that there are no leaks of fission products that could contaminate the reactor environment. Designed with dimensional tolerances appropriate to the project, fuel plates must undergo strict control and, for this reason, must be dimensionally characterized by obtaining accurate and reliable thickness data.

A dimensional deviation beyond the specified limits for fuel plate thickness could impact the minimum cladding thickness. Furthermore, if the thickness variations of the fuel plate exceed the specified limits, the assembly fit of the plates into the side plates of the fuel element may not be possible, considering the assembly tolerances (Durazzo and Riella, 2015). Therefore, the tolerances for fuel plate thickness depend on the minimum allowable cladding thickness and the dimensional tolerances of the spacing between the channels of the side plates of the fuel element.

At the Nuclear and Energy Research Institute (IPEN-CNEN/SP), the final dimensions of the fuel plate are determined by measuring its length, width, and thickness. The length is measured at 3 positions using a precision caliper with a resolution of 0.02 mm, and the width is measured at 7 positions using a precision micrometer with a resolution of 0.01 mm. Fuel plate thickness is measured at 21 positions using a u-shape frame micrometer with non-rotating spindles and chamfered measuring anvils as shown in Fig. 3. The resolution of the thickness measurements is 0.01 mm. The positioning of the instrument stops in relation to the plate coordinates is facilitated by a template made of

* Corresponding author. Av. Prof. Lineu Prestes, 2242, Cidade Universitária, CEP, 05508-000, São Paulo, SP, Brazil.
E-mail addresses: marcelo.k@ipen.br (M. Kobayoshi), lealneto@ipen.br (R.M. Leal Neto), elitaucf@ipen.br (E.F. Urano de Carvalho), thomaz@protolab.com.br (T.A.G. Restivo), mdurazzo@ipen.br (M. Durazzo).

https://doi.org/10.1016/j.pnucene.2024.105332
Received 9 November 2023; Received in revised form 25 April 2024; Accepted 14 June 2024
Available online 21 June 2024

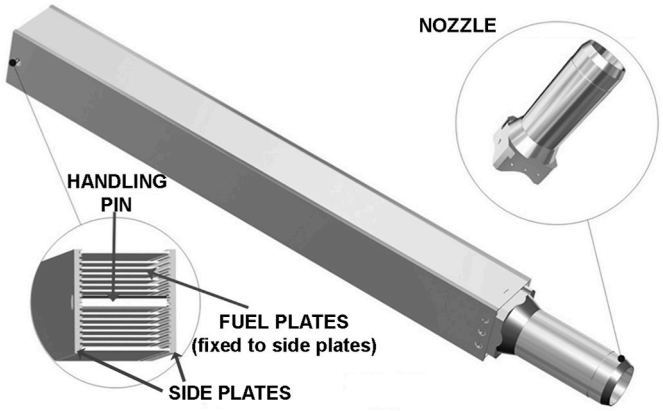

Fig. 1. MTR-type nuclear fuel element.

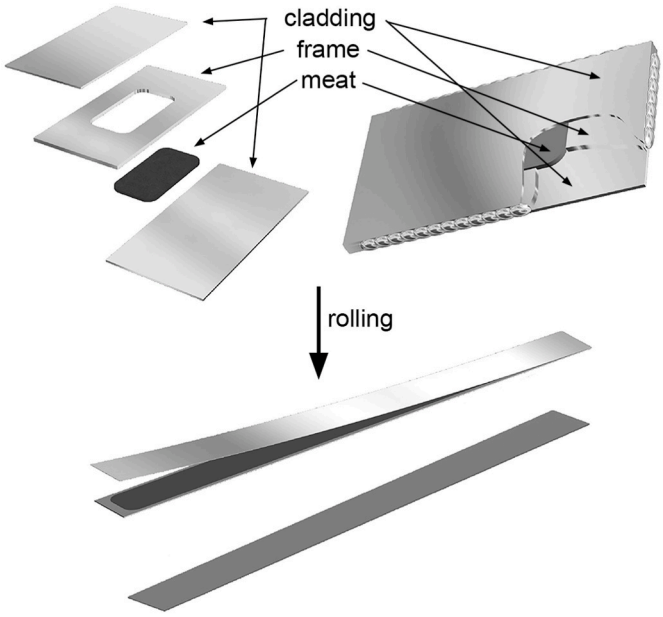

Fig. 2. Picture frame technique used to manufacture fuel plates.

Fig. 3. Measurement of fuel plate thickness at IPEN-CNEN/SP.

acrylic (polymethyl methacrylate). Fig. 4 provides a diagram illustrating the positions at which the fuel plate thickness measurements are taken. By measuring dimensions A, B, C, and D in the radiographic image, the centralization of the meat is ensured.

After operators read the instrument scales, the fuel plate thickness

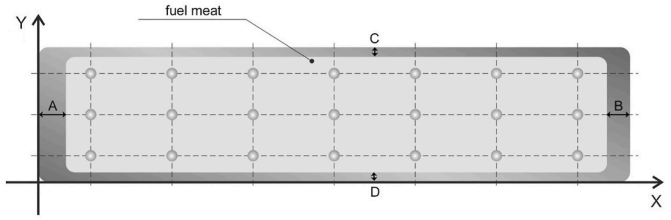

Fig. 4. Typical scheme for measuring the fuel plate thickness.

measurements are manually recorded on standardized forms following internal procedures. The average time for a trained operator to complete a measurement cycle at the 21 pre-established points on the fuel plate, including the subsequent time required for manually recording the values read from the instrument scale onto the standardized forms, is 20 min.

The current fuel plate thickness measurement method has several limitations and disadvantages. First, the use of manual measuring instruments inevitably introduces the human error into the control process. This can be caused by improper handling and positioning of the instruments, incorrect measuring readings, or error in transcribing the measured values onto the standardized form. All this can adversely affects the reliability of the results. Second, the current method is time-consuming, requiring an average of 20 min per measurement cycle. Third, the current method is unable to provide a quantitative analysis of the collected data due to the use of manual operations for measurements and transcriptions of results. The need for repeated measurements to establish a database for statistical analysis would further slowdown the process and make it prone to errors, significantly increasing its execution costs. Finally, the use of manual measuring instruments with mechanical contact can potentially damage the surfaces of fuel plates if handled improperly. This issue is exacerbated by the fact that the measuring surfaces of these instruments are typically manufactured from high-hardness materials to ensure greater resistance to abrasion and durability. In the case of the external micrometers used in the current method, their measuring anvils are made of tungsten carbide, with specified hardness levels between 88 and 93 HRa, equivalent to approximately 1100 HV (Tungsten Carbide Powder, 2008). This hardness value can be considered extremely high when compared to the material composition of the fuel plate cladding, which is Class 6061-T4 aluminum, with a hardness of around 65 HB, equivalent to approximately 70 HV (Matweb, 1999). Avoiding surface defects is advisable since experimental results suggest that corrosion points initiated in areas with surface defects can lead to the penetration of the cladding and result in the exposure of the meat, causing the release of fission products inside the reactor and leading to serious operational and safety issues (Durazzo and Riella, 2015).

For this reason, it was decided that the proposal for the new measurement method should also consider the design and construction of a measuring apparatus that could automatically make mechanical contact with the fuel plate through the application of a contact system with the ability to control and adjust the measuring force. Additionally, the new method should reduce the contact area of the measuring instrument with the plate's surface, considering that the external micrometers currently used have a 6.5 mm diameter on their contact faces.

Finally, the new measurement method should significantly increase the number of measuring points, allowing for the collection of more data for thickness analysis and a more detailed study of the influencing factors involved in the manufacturing process of the plates. It was also determined that the new proposal should include data outputs, enabling the creation of a response curve generated from the variation in plate thickness, allowing for a visual analysis of its characteristics.

To address these limitations, several proposals for improving the current method have been considered and implemented. The first proposal is to use automation technology to conduct the measurements.

This would eliminate the human factor from the process, reduce the measurement time, and enable quantitative data analysis. The second proposal is to design and construct a measuring apparatus that could automatically make mechanical contact with the fuel plate through the application of a contact system with the ability to control and adjust the measuring force. This would reduce the risk of damaging the fuel plate surface. The third proposal is to increase the number of measuring points, allowing for the collection of more data for thickness analysis and a more detailed study of the influencing factors involved in the manufacturing process of the plates. The use of a larger area in the case of using a micrometer with a micrometric head of 6.5 mm can lead to errors due to undetectable deviations, as well as errors due to the different pressures exerted on the plate surface. The new device would be an advancement in characterizing fuel plate thickness, enabling increased measurement discrimination by detecting localized thickness variations (local defects). The fourth proposal is to include data outputs, enabling the creation of a response curve generated from the variation in plate thickness, allowing for a visual analysis of its characteristics.

This work describes the development of a device and the associated method for the automated measurement of the thickness of nuclear fuel plates used in research reactors. The new measuring device offers several improvements over the previously used method, resulting in gains in efficiency, flexibility, and metrological reliability in the evaluation of the thickness compliance of fuel plates manufactured at IPEN-CNEN/SP.

2. Definition of measurements requirements

Defining the requirements for the measurement system was essential to start the project development, as the sizing of the entire mechanical, pneumatic, electrical, automation, and integration structure of the system would depend on their technical and operational characteristics. The following key technical parameters were considered in the design of the measurement system:

2.1. Fuel plate specifications

The measurement system must meet the metrological requirements of the products to be measured. Therefore, the geometric, dimensional, and tolerance characteristics of the fuel plates currently manufactured at IPEN-CNEN/SP were studied in detail. This was necessary to determine the decision rules for verifying the compliance or non-compliance of fuel plates according to their design specifications.

2.2. Displacement and measurement movements

The measurement system must be capable of translating along the X, Y, and Z Cartesian axes to accommodate the spatial movement required for length, width, and thickness measurements of the fuel plates. The displacement along the Z-axis is the most critical, as it is used for thickness measurements, which have the tightest dimensional tolerance among the fuel plate characteristics.

To ensure its accuracy and precision, Z-axis displacement was integrated directly into the sensors, using an automated movement system for their measuring spindles.

2.3. Speeds of displacement and measurement

The speeds and acceleration ramps of displacement and measurement are directly related to the number of readings per unit of time that the system can perform. Therefore, establishing these speeds is essential for determining the future measurement times and sizing various components of the system. It was established that the measurement system should be able to achieve a displacement speed between measurement points of up to 100 mm/s, and that these speeds and acceleration ramps could be determined through programming.

2.4. Laboratory environment

The new measurement system will be installed within the metrology laboratory at IPEN-CNEN/SP, which already has a temperature and relative humidity control system in place. This allows for maintaining temperature gradients within acceptable limits for dimensional control of the fuel plates. Despite the existence of these systems, the specifications regarding the limits of variation in measurements due to potential temperature gradients in the environment were considered crucial for the project and the selection of materials for manufacturing the system components.

2.5. Signal integration

The chosen components of the measurement system must be compatible with the other components envisaged in its design, considering the types of signals and communication protocols that can be applied, as well as the future needs for adapting to communication standards and data processing.

2.6. Structure of the measurement system

The physical characteristics related to the size, shape, and weight of the measurement system were also considered when determining the most suitable measuring sensor. Therefore, the chosen measuring sensor should be compact enough to be installed in the proposed model during the system's conceptual phase, and it should have the smallest possible mass to minimize deformations in the rigid elements of the system and mitigate the effects of inertial forces acting on the moving parts.

3. Design and construction of the equipment and data processing

The experimental development of the study led to the conception, design, and construction of a technological apparatus, subsequently named "Equipment for Automated Measurement of Fuel Plates using Sensors based on Optical Linear Encoders". After the equipment was constructed, functional tests were conducted, and four fuel plates were effectively measured.

3.1. Definition of measuring sensors

Various types of dimensional measurement sensors were studied, which could operate both with and without mechanical contact between the sensor and the plate. These sensors were based on different measurement principles, including ultrasonic, pneumatic, resistive, magnetic, inductive, capacitive, and optical systems.

Based on the defined measurement requirements and the functional and metrological characteristics of sensors using different measurement principles, we sought to determine the most suitable type of sensor for the project.

The functional and project specifications of each alternative were analyzed, including their dimensions, measurement ranges, resolution, maximum permissible errors (Mpe), repeatability, response speed, and, most importantly, sensitivity to known influencing factors in the operational environment of the measurement system.

Structural and application aspects were also considered, such as the spatial suitability of each sensor, robustness, methods of fixation, data presentation formats, as well as possibilities for connectivity, integration, and presentation of results. Table 1 provides an analysis of measuring sensors from the perspective of their operation in the measurement system to be developed. They are rated on a scale from 1 to 5, where 1 represents poor and 5 signifies excellent.

Table 1 demonstrates that optical-based sensors are the superior choice. After careful technical, technological, and financial considerations, it was decided that optical sensors based on optical linear

Table 1
Summary of the analysis of measurement sensor characteristics.

Characteristics[a]	Measurement Principle						
	ultrasonic	pneumatic	resistive	magnetic	inductive[b]	capacitive	optical[c]
dimensions	3	1	2	3	5	1	5
measuring range	4	1	3	5	4	4	5
resolution	4	4	5	4	5	5	5
accuracy	3	4	2	3	5	3	5
repetitiveness	2	3	1	2	4	3	4
response speed	5	4	2	2	4	4	5
influencing factors	1	5	4	3	3	2	4
mechanical adaptability	1	1	3	3	5	2	5
electronic adaptability	1	3	5	4	5	1	5
Total	**2.67**	**2.89**	**3.00**	**3.22**	**4.44**	**2.78**	**4.78**

[a] Analyzed in relation to the measurement system to be developed.
[b] Based on differential inductive systems using Mutual Inductance (LVDTs).
[c] Based on optical systems using linear encoding (OLE) and laser triangulation.

encoder systems (OLE) would be the best choice for integration into the project. An additional factor contributing to this decision was the realization that certain models of these sensors could incorporate features for automatic movement of their spindles and provide suitable connectivity solutions for data capture and transmission to the system.

The Linear Encoder-Based Measurement Sensors (OLE), Mitutoyo LGB-2 model, with a measuring range of 10 mm, resolution of 1 μm, and maximum permissible error (M_{PE}) of 2 μm were selected, operating in conjunction with the integrated indication and communication module Mitutoyo EH-102P, with a deviation (quantization error) of ±1 significant digit, which in our case corresponds to ±1 μm.

3.2. Equipment design

In the development of the equipment's design, various structural factors were considered, such as:

- Reference system: the reference system provides a fixed reference point for the measurement system.
- Rigidity of the assembly: the assembly must be rigid enough to prevent deformation during measurement, which could introduce errors.
- Degrees of freedom of the plate under measurement: the plate must be held in place securely during measurement, but it must also have enough degrees of freedom to allow the measurement system to access all of the desired measurement points.
- Contact methods: the measurement system must make contact with the plate in a way that does not damage the plate or introduce errors into the measurement.
- Fixation system: the fixation system must hold the plate in place securely during measurement, but it must also be easy to load and unload the plate.
- Positioning of heating sources in the system: heating sources must be positioned in a way that does not introduce temperature gradients into the system, which could affect the accuracy of the measurements.
- Parallax errors.
- Abbe errors (errors arising from the misalignment between the instrument scale and the object being measured).
- Anticipated angular deviations.

Fig. 5 illustrates the initial conception of the equipment.

Based on this initial conception, work was carried out to develop the project for a device that should consist of:

- A movement system, based on displacement motors controlled by a programmable logic controller (PLC).

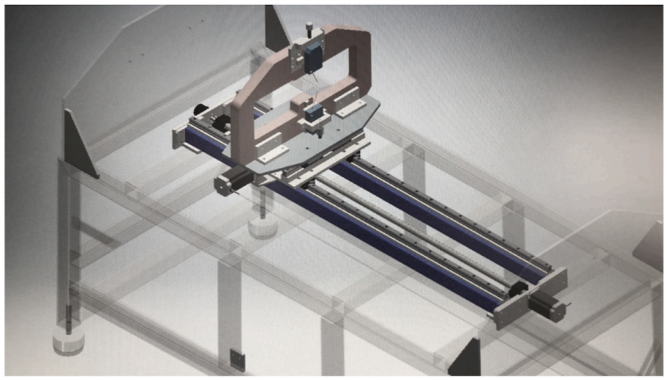

Fig. 5. Initial conception of the equipment.

- A data acquisition and processing system, composed of measurement sensors, optical fiber tangency detectors, linear displacement transducers, a computer, and result analysis software.

For the development of the project and the generation of related manufacturing and assembly drawings, computer-aided design (CAD) software Inventor®, developed by Autodesk®, Inc., was used.

The structural design of the equipment was oriented towards performing thickness measurements of fuel plates through the movement in the X and Y plane of two linear measurement sensors based on the optical principle of photoelectric transmission (OLE), acting differentially.

For a better understanding, the subassemblies and components that make up the equipment are described below, with reference to the numbers shown in Fig. 6.

The subassembly of the measuring arc, also known as the scanning gantry (9), is supported on the linear conveyor of the X-axis (6), whose movement is carried out by the stepper motor (7), and its translation coordinates are captured by the linear transducer of the X-axis (8).

This assembly, in turn, is mounted on the conveyors of the Y-axis (3), whose displacement is controlled by the servo motor (4), and their translation coordinates are captured by the linear transducer of the Y-axis identified by number (5).

All of this assembly is supported by a structural steel base (1) that is placed on the ground with the use of anti-vibration dampers (2), ensuring rigidity and stability to the equipment.

On this same structural base, the crossbars of the positioners (10) are also fixed, where the linear motion guides of the positioners (11) are located. These guides support the fixed positioner (13), the limiting stop (12), and the spring-loaded positioners (14), which are part of the stand for measuring the fuel plate (15).

The items that make up the assembly of the measuring arc

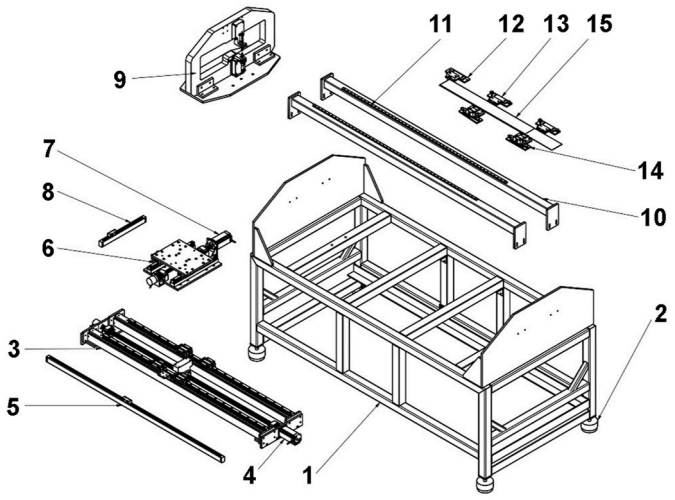

Fig. 6. Exploded view of the subassemblies and components of the equipment.

subassembly, identified as (9) in Fig. 6, are described below, related to the numbers highlighted in Fig. 7.

The two opposing linear photoelectric transmission measurement sensors (21 and 28) and the emitter (25) and receiver (31) of the optical fiber sensor are mounted on the height adjustment brackets of the sensors (19 and 20). These height adjustment brackets, in turn, are fixed to the rigid structure, manufactured as a single body, called the aluminum arc (16), which is supported on a base (17) and secured using angle brackets (18).

3.3. Manufacture of the equipment

Once the construction and functional designs of the equipment were completed, the manufacturing process began, including the construction of the base, machining of the parts, assembly of subassemblies and components, and initial adjustments and adjustments.

For the construction of the equipment base, square-section tubular elements of 50 mm × 50 mm and 30 mm × 30 mm, 1 ½ inch angles, and 15 mm thick rolled steel plates, all made of SAE 1045 steel, were used. The elements were joined by arc welding with inert gas shield MIG (Metal Inert Gas Welding), followed by grinding and surface protection with the application of a 40 μm layer of matte-textured acrylic polyurethane-based catalyst product.

For machining the more complex parts, the project models generated in CAD were used, and the data was directly imported into the computer-aided manufacturing (CAM) software Edgecam™, developed by Hexagon Manufacturing Intelligence™. This software conducted machining analysis and programmed instructions for computer numerical control (CNC) of the machine tools.

The manufacturing operations of the rotating parts were carried out on the Romi® GL 240 turning center equipped with the GE 0i-TC™ control system developed by Fanuc Corporation™. The prismatic parts were manufactured on the Romi® D 600 vertical machining center, equipped with the Sinumerik 828D™ control system developed by Siemens Aktiengesellschaft™.

Less complex machining operations were performed on conventional machine tools such as horizontal lathes, universal milling machines, horizontal milling machines, surface grinders, cylindrical grinders, and column and bench drills.

After completing the machining of the parts, the assembly of the equipment began with the base, fixing the supporting elements, linear motion guides, and the placement of the Y-axis ball screw.

Next, the subframe assembly was carried out, fixing the linear motion guides, placing the X-axis ball screw, followed by fixing the support base and mounting the measurement arc.

The crossbars for the positioners were fixed, and the limiting stop, fixed positioner, and spring-loaded positioners of the plate measuring stand were installed.

Motor couplings to the ball screws and the installation of position detectors, limit switches, optical fiber sensors, and measurement sensors were performed.

During the assembly of the components, various adjustments were made to ensure maximum equipment accuracy, minimizing geometric errors associated with its operation and thus guaranteeing the accuracy of the results.

The manufacturing process was completed with the positioning and wiring of the electro-electronic and electropneumatic components, including power supplies, programmable logic controller (PLC), human machine interface (HMI), switches, drive, control, and communication modules, control switches, and other protection switches and components. Fig. 8 shows the equipment in the final assembly phase.

3.4. Systems integration

Once the mechanical components were assembled, adjusted, and regulated, the processes of electro-electronic, electropneumatic, and data integration began through the interconnection between the PLC of the measurement system and the other designated hardware and software, as well as the development and implementation of the data acquisition network and the standardization of the sensor signal transmission. In this integration, communication between the PLC, the HMI, and the processing system was established through the use of a switch via an Ethernet local area network (LAN), as shown in the diagram in Fig. 9.

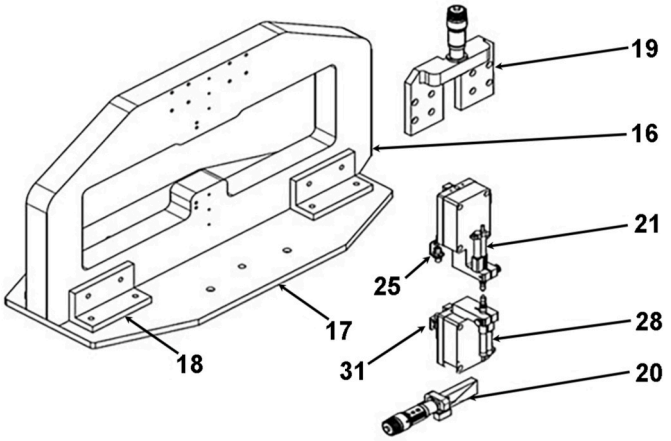

Fig. 7. Exploded view of the measuring arc subassembly.

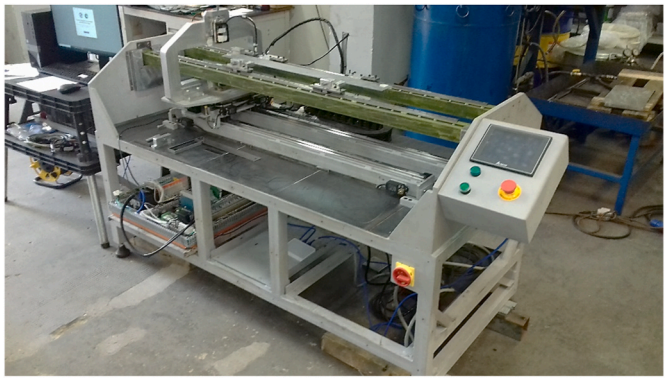

Fig. 8. Equipment in the final assembly phase.

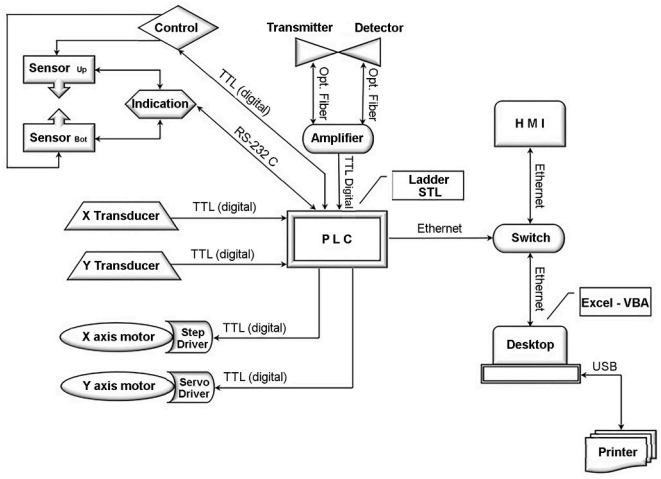

Fig. 9. Signal integration diagram.

3.5. Functional tests and measurements

After completing the manufacturing and integration stages of the equipment, various functional tests were conducted, including the execution of activation commands and verification of movement responses, as well as the transmission and reception of signals.

With the successful execution of an extensive series of movement tests and data transmission checks, the equipment was considered integrated and compliant with the project's requirements. It was declared ready for calibration and for use in real measurement situations.

Once the system was operational according to the project, calibrations and tests in real measurement conditions began. The behavior of the system in the processes of data generation, transmission, collection, and processing was observed.

After its calibration, the validation of the proposed method was performed based on the results obtained from the equipment. This involved analyzing the reliability and integrity of data transmission across the network.

Following its installation in the metrology laboratory and preparation for the start of measurements on different types of fuel plates routinely manufactured at IPEN-CNEN/SP, the development of the data treatment model began, as described in the following section. Fig. 10 illustrates the completed equipment, ready for use, installed in the metrology laboratory.

4. Mathematical data treatment

The mathematical treatment of the data obtained in the measurements was guided by the creation of a mathematical model, based on statistical studies and the analysis of influencing factors in the system. Its development was based on the methodology expressed in the document JCGM 100:2008 - Evaluation of Measurement Data - Guide to the Expression of Uncertainty in Measurement - known by the acronym GUM (JCGM, 2008), which is adopted by international organizations such as Bureau International des Poids et Mesures (BIPM), International Electrotechnical Commission (IEC), International Federation of Clinical Chemistry (IFCC), International Organization for Standardization (ISO), International Union of Pure and Applied Chemistry (IUPAC), International Union of Pure and Applied Physics (IUPAP), and International Organization of Legal Metrology (OIML).

Fig. 10. Completed equipment ready for use.

The following example uses real data from thickness measurements of the fuel plate with serial number Si-1099, manufactured at IPEN-CNEN/SP to compose a fuel element for use in the IEA-R1 research reactor.

This same mathematical treatment was later programmed and validated using Microsoft Excel® software with the addition of Visual Basic for Applications (VBA), which performs the same processing and analysis on all measured thickness points of the plates, applying identical mathematical rigor as presented below.

4.1. Mathematical modeling

Initially, the modeling of the measurement phenomenon was developed with the aim of mathematically expressing the relationship between the output Y and the input variables Xi, of which Y has a functional relationship f, in the form:

$$Y = f(X_1, X_2, X_3, \ldots, X_n) \tag{1}$$

In the proposed method, the thickness of the fuel plate is determined by comparison with the thickness of a previously calibrated reference standard block with the same nominal thickness. The direct output of the comparison between the measurement of the block and the plate will be the difference in their thicknesses, that is:

$$E_{pla} = E_{pad} + \Delta E_{p-p} \tag{2}$$

where:

E_{pla} = thickness of the plate under measurement.

E_{pad} = thickness of the reference standard block.

$\Delta E_{p\text{-}p}$ = difference between the thicknesses of the plate and the reference standard block.

Thus, starting from Eq. (1), we sought to determine the functional relationship between the measurand (plate thickness) and the other input quantities that could contribute an uncertainty component to the measurement result. This analysis was based on the following points:

a) Knowledge of structural data of the equipment;
b) Information about the calibration standards used;
c) Technical data obtained from manufacturers of its components;
d) Tests conducted during the manufacturing and assembly of the equipment;
e) Environmental information about the location of installation and operation of the equipment.

Thus, the following mathematical measurement model was established:

$$E_{pla} = E_{pad} + \Delta E_{p-p} + \delta S_{sup} + \delta S_{inf} + \delta R_{ind} + \delta T_{ref} + \delta T_{p-p} + \delta F_{sup} + \delta F_{inf} + \delta P_{gui} + \delta A_{pla} + \delta A_{p-p} \tag{3}$$

where:

E_{pla} = Thickness of the plate under measurement.

E_{pad} = Thickness of the reference standard block.

$\Delta E_{p\text{-}p}$ = Difference between the thicknesses of the plate and the

reference standard block

δS_{sup} = Correction due to the maximum permissible error of the upper sensor

δS_{inf} = Correction due to the maximum permissible error of the lower sensor

δR_{ind} = Correction for the effect of the resolution of the integrated indication module

δT_{ref} = Correction for the effect of deviation from the reference temperature

$\delta T_{p\text{-}p}$ = Correction for the effect of the temperature gradient between the standard and the plate

δF_{sup} = Correction for the effect of the measuring force of the upper sensor

δF_{inf} = Correction for the effect of the measuring force of the lower sensor

δP_{gui} = Correction for the parallelism deviation between the equipment's guides

δA_{pla} = Correction for the alignment deviation between the plate and the movement

$\delta A_{p\text{-}p}$ = Correction for the alignment deviation between the plate and the reference standard.

4.2. Calculation of measurement results

As previously mentioned, independent measurements were considered, obtained under repeatability conditions, of the thickness of the fuel plate with serial number Si-1099 at the intersection point of coordinates X = 35.00 mm and Y = 112.50 mm. The results are presented in Table 2.

From the data presented in Table 2, the measurement result, i.e., the estimate y of the measurand Y, was calculated using the functional relationship f, with the estimates x_i obtained for the input quantities X_i. It was assumed that the best available estimate of the expected value μy of a quantity y that varies randomly is the arithmetic mean $\bar{y}$ of the n observations, as follows:

$$\bar{y} = \frac{1}{n}\sum_{i=1}^{n} y_i = 1.524\ mm \tag{4}$$

4.3. Evaluation of uncertainty contributions

Table 3 presents the input quantities, their estimated values, their standard uncertainties, their sensitivity coefficients, and their respective uncertainty contributions as calculated.

Based on the obtained results, it can be observed that the input quantities associated with the deviations in parallelism between the equipment guides (δP_{gui}), alignment between the plate and the movement (δA_{pla}), and alignment between the plate and the reference ($\delta A_{p\text{-}p}$) did not contribute significantly to the uncertainty in comparison to the others.

Therefore, for the purpose of reducing the volume of data analysis in the software, it was decided to disregard them in defining the final mathematical model for performing the uncertainty analysis calculation of measurement results.

Therefore, the mathematical measurement model described in Eq. (3) becomes:

$$E_{pla} = E_{pad} + \Delta E_{p-p} + \delta S_{sup} + \delta S_{inf} + \delta R_{ind} + \delta T_{ref} + \delta T_{p-p} + \delta F_{sup} + \delta F_{inf} \tag{5}$$

4.4. Evaluation of associated covariances

By evaluating the presence of associated covariances between input estimates (Eq. (5)), it is concluded that there is no significant correlation between them. In other words, the inputs can be considered independent from each other, and therefore, the expression for the combined variance u^2c (y) associated with the measurement result will be:

$$u_c^2(y) = \sum_{i=1}^{N}\left[\frac{\partial f}{\partial x_i}\right] u^2(x_i) \tag{6}$$

4.5. Determination of the combined standard uncertainty

The contributions of uncertainty were then combined as follows:

$$u_c(y) = u_c\left(E_{pla}\right) = \sqrt[2]{\left(\begin{array}{c} 0.00045^2 + 0.00006^2 + 0.00100^2 + 0.00100^2 + 0.00050^2 + 0.00032^2 + \\ 0.00006^2 + 0.00026^2 + 0.00026^2 \end{array}\right)} u_c\left(E_{pla}\right) = 0.00164\ mm \tag{7}$$

4.6. Determination of expanded uncertainty

Next, the calculation of the effective degrees of freedom ν_{eff} was performed based on the degrees of freedom ν_i of individual uncertainty contributions $u_i(y)$, using the Welch-Satterthwaite formula as follows:

$$\frac{u_c^4(y)}{\upsilon_{eff}} = \sum_{i=1}^{N}\frac{u_i^4(y)}{\upsilon_i} \tag{8}$$

Which can be rewritten as:

$$\upsilon_{eff} = \frac{u_c^4(y)}{\sum_{i-1}^{N}\frac{u_i^4(y)}{\upsilon_i}} = \frac{0,00164^4}{\frac{0.00045^4}{9}} = 1.567 \tag{9}$$

Then, with the effective degrees of freedom ν_{eff} for the combined standard uncertainty u_c (E_{pla}) obtained, the coverage factor k was determined using the Student's t -distribution assuming a coverage probability of 95%, as follows:

$$k_p = t_p\left(\vartheta_{eff}\right)$$

$$k_{95} = t_{95}(1.567) = 2.0 \tag{10}$$

So, considering the Central Limit Theorem, it is sufficient to assume that the probability distribution (y-Y)/$u_c(y)$) is the t-distribution and take $k_p = t_p$ (ν_{eff}), with the t-factor based on the number of effective degrees of freedom obtained from the Welch-Satterthwaite equation [7].

Therefore, the expanded uncertainty is obtained as:

Table 2
Results obtained for the plate Si-1099 in a real measurement situation.

Repetition	Obtained Value (mm)
1	1.524
2	1.523
3	1.524
4	1.524
5	1.524
6	1.524
7	1.523
8	1.524
9	1.527
10	1.527

Table 3
Evaluation of uncertainty contributions.

Input Quantity X_i	Estimated Value of Quantity x_i	Standard Uncertainty $u(x_i)$	Probability Distribution	Sensitivity Coefficient $\|c_i\|$	Uncertainty Contribution (mm) $u_i(y)$
ΔE_{p-p}	0.024	$4.52*10^{-04}$	normal	1	0.00045
E_{pad}	1.500	$6.00*10^{-05}$	normal	1	0.00006
δS_{sup}	0	$1.00*10^{-03}$	normal	1	0.00100
δS_{inf}	0	$1.00*10^{-03}$	normal	1	0.00100
δR_{ind}	0	$5.00*10^{-04}$	normal	1	0.00050
δT_{ref}	0	$8.66*10^{-01}$	rectangular	$3.65*10^{-04}$	0.00032
δT_{p-p}	0	$1.73*10^{+00}$	rectangular	$3.53*10^{-05}$	0.00006
δF_{sup}	0	$5.77*10^{+01}$	"U" type	$4.51*10^{-06}$	0.00026
δF_{inf}	0	$5.77*10^{+01}$	"U" type	$4.51*10^{-06}$	0.00026
δP_{gui}	0	$1.04*10^{-04}$	"U" type	$4.41*10^{-04}$	0.00000
δA_{pla}	0	$3.79*10^{-04}$	"U" type	$1.61*10^{-03}$	0.00000
δA_{p-p}	0	$7.07*10^{-04}$	"U" type	$3.00*10^{-03}$	0.00000

$$U_p = u_c(y) * k_p$$

$$U_{95}(E_{pla}) = u_c(E_{pla}) * k_{95}$$

$$U_{95}(E_{pla}) = 0.00164 * 2.0 \cong 0.003\,mm \tag{11}$$

4.7. Report of measurement results

Finally, it is possible to declare the measurement result for the measured point as follows:

$$(1.524 \pm 0.003)\,mm \tag{12}$$

The reported measurement uncertainty is declared as the expanded uncertainty, i.e., the standard uncertainty of the measurement multiplied by the coverage factor $k = 2.0$, which, for a t-distribution with $\nu_{eff} = 1.567$ effective degrees of freedom, corresponds to an approximate coverage probability of 95%.

5. Execution of measurements

Once functional tests were completed, and data processing methods were developed and programmed, a series of measurements began in the laboratory conditions. The goal was to obtain proof of the metrological reliability of the equipment. These initial measurements aimed to observe the equipment's performance, evaluate the results, and assess the stability, drift, and instrumental bias of the system. Systematic analysis of the uncertainty in the results was carried out using the presented mathematical model.

To validate the new measurement system, two plates with manufacturing codes Si-1097 and Si-1099, manufactured for use in the IEA-R1 research reactor, were made available by IPEN-CNEN/SP. Additionally, two plates with manufacturing codes IPMB-007 and IPMB-010, manufactured for use in the IPEN/MB-01 research reactor, were also provided.

The equipment allows defining the number of points at which each fuel plate can be measured. These points are located according to their coordinates on the plate's plane. The sum of these points is referred to as the number of measured points (N_p).

The number of measured points results from a measurement matrix adopted on the X and Y axes of the system. This matrix consists of a number of columns (N_X) identified by their coordinates on the X-axis (width of the plate) and a number of rows (N_Y) identified by their coordinates on the Y-axis (length of the plate).

When all the measurement points determined by the matrix are measured, one measurement cycle is completed. To perform a statistical analysis of the collected data, repetitions of these cycles are executed. The number of these repetitions (N_c) determines the sample size obtained at each of the measured points.

Carrying out all the predefined measurement cycles allows for the development of calculations to present the plate's thickness results and characterizes a complete measurement series with (N_d) collected data.

5.1. In summary

$$N_X * N_Y = N_p \tag{13}$$

where:
N_X = Number of columns.
N_Y = Number of rows.
N_p = Number of measured points
and,

$$N_p * N_c = N_d \tag{14}$$

where:
N_p = Number of measured points.
N_c = Number of complete cycles.
N_d = Number of collected data.

For the purpose of providing future analysis and comparisons, in these initial measurements, it was chosen to collect data at the same positions determined by the previous procedure, which guide manual measurements using micrometers. Thus, measurements were made on the four available plates, as presented in Table 4.

6. Results and discussion

The measurement results obtained by the equipment are summarized in Table 5.

After each measurement, the equipment automatically generates a measurement report accompanied by chromatic response curves showing the variation in plate thickness. Examples taken from plate Si-1099 are provided. Fig. 11 shows the perspective response curve of the

Table 4
Series of thickness measurements performed.

Fuel Plate	Number of Points Measured per Cycle (N_p)	Number of Cycles Conducted (Sampling – N_c)	Number of Data Collected (N_d)
Si-1097	21	5	105
Si-1099	21	5	105
IPMB-007	21	5	105
IPMB-010	21	5	105
Total		20	420

Table 5
Results of the measurements performed at 21 points with 5 repetitions.

Fuel Plate	Minimum Thickness (mm)	Average Thickness (mm)	Maximum Thickness (mm)	Uncertainty (mm)
Si-1097	1.470	1.484	1.498	±0.003
Si-1099	1.498	1.533	1.551	±0.003
IPMB-007	1.355	1.362	1.366	±0.003
IPMB-010	1.349	1.358	1.368	±0.003

Si-1099 fuel plate evaluated at 21 points. Fig. 12 presents the same response curve in plan view.

In addition to the measurements on the four plates, the equipment's precision was also studied by checking its repeatability. At the beginning of each measurement series, a sensor adjustment (or preset) was performed using a reference standard block of "Grade 0" (JIS, 2004), with a thickness equal to the nominal thickness value of the fuel plate type to be measured. After completing the first cycle of measurements and in all subsequent cycle repetitions of the series, the equipment received a command to return to the sensor adjustment point, where the device's response value in indicating the thickness of the standard block was verified.

This verification was performed a total of 218 times, with the largest variation found in relation to the adjustment value made at the beginning of each series being 2 μm. This value was assumed to be the repeatability (precision) of the equipment.

The development of an approach introducing measurement uncertainty as a parameter to express measurement variability has had a significant impact on the decision-making process regarding whether to accept a product or not. This approach implies the need to consider comparison through a probabilistic perspective (Ribeiro and Gölze, 2017).

The ISO 14253–1:2017, UKAS LAB-48:2022, and ASME B89.7.3.1:2001 standards establish rules for verifying compliance or non-compliance with a specific tolerance for a feature of a workpiece, taking into account the measurement uncertainty (ISO, 2017; UKAS, 2022; ASME, 2001). Fig. 13 illustrates this relationship.

Similarly, the guiding document JCGM 106:2012, known as Supplement 6 to the GUM, provides comprehensive standardization of procedures to be used for verifying the conformity of items with specified requirements. It extensively covers the use of measurement results to decide, through acceptance or rejection, whether an item of interest meets a specified requirement (JCGM, 2012).

Based on the results obtained from the measurements conducted and considering the guiding document JCGM 106:2012, the measurement capability index C_m of the equipment was determined using the following equation:

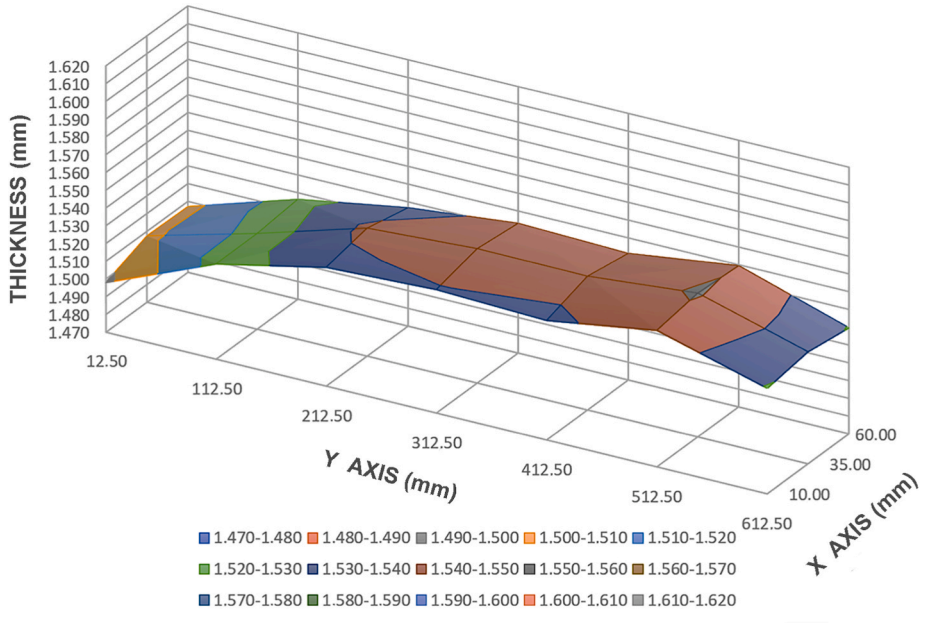

Fig. 11. Response curve of fuel plate Si-1097 evaluated with 21 points - Perspective.

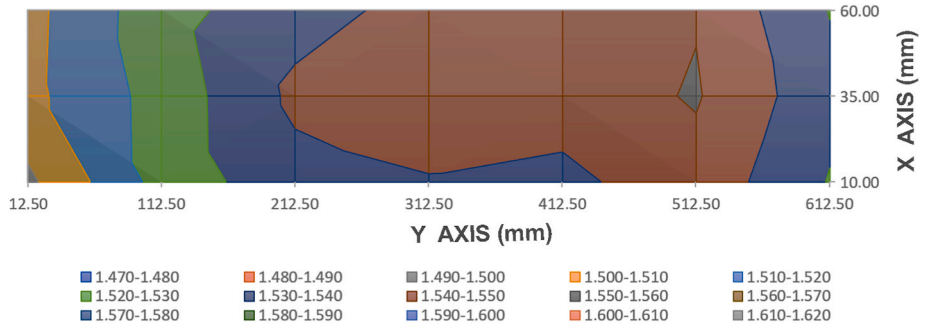

Fig. 12. Response curve of fuel plate Si-1097 evaluated with 21 points – Plan View.

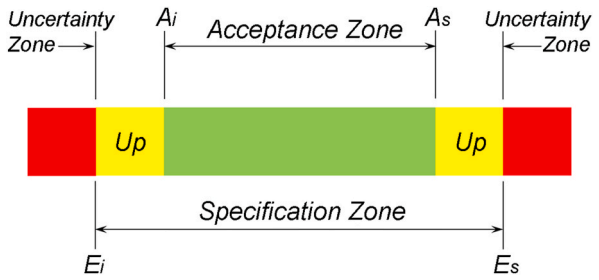

Fig. 13. Conformity acceptance limits.

$$C_m = \frac{E_s - E_i}{4u_c} = \frac{I_E}{2U_{95}} \tag{15}$$

where:

E_s = Upper specification limit.
E_i = Lower specification limit
u_c = Combined measurement uncertainty.
I_E = Specification interval.
U_{95} = Expanded uncertainty ($k = 2.0$).

It is assumed in this equation that the distribution of the obtained values follows a probability density function represented by a Gaussian curve, where the coverage probability for this interval is approximately 95%. Therefore, the measurement capability indices of the equipment were calculated, as presented in Table 6.

An analysis of Eq. (15) makes it clear that the measurement capability indices obtained are directly related to the values of the combined standard uncertainties u_c obtained in the results. Therefore:

$$\text{if } C_m \geq 5 \rightarrow u_c \leq \frac{I_E}{20} \tag{16}$$

Certainly, using the same reasoning and assuming that the distribution of values obtained in measurements follows a Gaussian probability density function, where the probability of coverage for such an interval is approximately 95%, we can conclude that:

$$\text{if } C_m \geq 5 \rightarrow U_{95} \leq \frac{I_E}{10} \tag{17}$$

In this case, C_m values equal to or greater than 5 indicate that the expanded uncertainties obtained from the measurement results produced by the equipment were always equal to or less than 10% of the value of the specification limits (tolerance) for the measured dimensions of the fuel plate.

Another point to highlight is that the repeatability value of 2 μm (0.002 mm) is consistent and aligns well when correlated with the maximum quantization error of the sensor system specified by the manufacturer, which is ±0.001 mm.

The repeatability also appears congruent when correlated with the values extracted from the uncertainty calculations for measurements of fuel plates Si-1097, Si-1099, IPMB-007, and IPMB-010, as presented in Table 7.

For the purpose of comparison, the expanded uncertainties U_{95} resulting from the current measurement method adopted at IPEN-CNEN/SP using micrometers reach the value of ±0.015 mm.

It is important to note that there is a significant difference in the thickness tolerances of fuel plates manufactured at IPEN-CNEN/SP, depending on the reactor in which they will be used. For the IEA-R1 fuel plate, the interval is 0.15 mm, while for the IPEN/MB-01 fuel plate, this interval is 0.04 mm.

Therefore, considering the acceptance criteria determined by IPEN-CNEN/SP, it is observed that the uncertainty value found with the current method using micrometers is acceptable for thickness measurement of plates for use in the IEA-R1 reactor. However, this same uncertainty value is entirely inadequate for the specified tolerances for plates manufactured for the IPEN/MB-01 reactor, as summarized in Table 8.

Table 6
Measurement capability indices of the equipment.

Fuel Plate	Specification Interval I_E (μm)	2 x Expanded Uncertainty $2 * U_{95}$ (μm)	Measurement Capability Index C_m
Si-1097	150	6.74	22.26
Si-1099	150	6.43	23.33
IPMB-007	40	6.62	6.04
IPMB-010	40	6.97	5.74

Table 7
Data from uncertainty calculation for measurements.

Fuel Plate	Combined Standard Uncertainty U_c (μm)	Effective Degrees of Freedom ν_{eff}	Coverage Factor k	Expanded Uncertainty U_{95} (mm)
Si-1097	1.71	178	1.97	±0.003
Si-1099	1.64	725	1.96	±0.003
IPMB-007	1.68	278	1.97	±0.003
IPMB-010	1.76	106	1.98	±0.003

7. Conclusions

The presented results demonstrate that the developed measurement equipment exhibits adequate precision, maintaining a value of 2 μm under repeatability conditions. This value also indicates the system's good stability and minimal bias.

In the measurements carried out on the four available plates, the uncertainty values in the results remained constant at around ±3 μm, indicating that the accuracy, resolution, and sensitivity of the equipment meet the dimensional control requirements.

Furthermore, the analysis of the obtained data, by relating the values of standard combined uncertainties U_c, effective degrees of freedom ν_{eff}, and coverage factors k, with the number of repetitions, confirms the appropriate mathematical modeling and demonstrates the correct correlations with influencing factors. This reveals a good understanding of the phenomena involved in the measurements.

Hence, it is evident that the goal of constructing equipment for programmable measurements, in which data can be automatically collected and processed, and results can be presented with their respective measurement uncertainties in the form of descriptive reports, graphs, and response curves, has been achieved.

Initial analyses indicate that in all measurements, measurement capability indices equal to or greater than five ($C_m \geq 5$) were achieved. This means that the expanded uncertainties obtained in the measurement results were always equal to or less than 10% of the specified thickness limits for the analyzed fuel plates.

Regarding analysis speed, the average time for a complete measurement cycle using a 3 × 7 matrix (21 points per cycle) decreased from

Table 8
Measurement capability indices from the external micrometer measurement of the fuel plates (for comparison with Table 6).

Reactor	Specification interval (thickness tolerance) I_E (μm)	2 x Expanded Uncertainty 2 x U_{95} (μm)	Measurement Capability Index C_m
IEA-R1	(1.620–1.470) = 150	(2 × 15) = 30	5.00
IPEN-MB-01	(1.370–1.330) = 40	(2 × 15) = 30	1.33

20 min in the previous (manual) method to 3 min and 20 s with the new equipment.

Therefore, the development of this new equipment has provided several advantages over previously used methods, resulting in efficiency, flexibility, and metrological reliability gains in the process of evaluating the thickness conformity of fuel plates manufactured at IPEN-CNEN/SP.

CRediT authorship contribution statement

Marcelo Kobayoshi: Data curation, Methodology, Resources, Validation. **Ricardo Mendes Leal Neto:** Data curation, Formal analysis, Investigation, Writing – review & editing. **Elita Fontenele Urano de Carvalho:** Data curation, Visualization. **Thomaz Augusto Guisard Restivo:** Formal analysis, Writing – original draft. **Michelangelo Durazzo:** Conceptualization, Formal analysis, Methodology, Project administration, Supervision.

Declaration of competing interest

The authors declare that they have no known competing financial interests or personal relationships that could have appeared to influence the work reported in this paper.

Data availability

Data will be made available on request.

Acknowledgments

The authors are grateful to São Paulo Research Foundation (FAPESP) for the research grant 2021/14331-5.

References

ASME, 2001. American society of mechanical engineers. In: Guidelines for Decision Rules Considering Measurement Uncertainty in Determining Conformance to Specifications, vol 2001. ASME, New York, p. 24. ASME B89.7.3.1-2001.

Cunningham, E., Boyle, E.J., 1955. MTR-Type fuel elements. Geneva, 8-20 August. In: International Conference on Peaceful Uses of Atomic Energy, 9, pp. 203–207, 1955.

Durazzo, M., Riella, H.G., 2015. Procedures for Manufacturing Nuclear Research Reactor Fuel Elements. OmniScriptum GmbH & Co, KG, Saarbrücken, Germany, 2015.

ISO, 2017. International Organization for Standardization. Inspection by measurement of workpieces and measuring equipment. Part 1: decision rules for verifying conformity or nonconformity with specifications, 3 ed. Geneva, 2017 Geometrical product specifications (GPS) 23. ISO 14.253-1.

JCGM, 2012. Joint committee for guides in metrology. Working group 1. Evaluation of measurement data: the role of measurement uncertainty in conformity assessment. Sèvres, 2012, 57 pp. JCGM 106:2012.

JCGM, 2008. Joint committee for guides in metrology. Working group 1. Evaluation of measurement data: guide to the expression of uncertainty in measurement. Sèvres, 2008 134. JCGM 100:2008. https://www.bipm.org/documents/20126/2071204/JCGM_100_2008_E.pdf.

JIS, 2004. Japanese Industrial Standards. Gauge Blocks, 2004. Japanese Standards Association, Tokyo, p. 39. JIS B 7506.

Kaufman, A.R., 1962. Nuclear Reactor Fuel Elements, Metallurgy and Fabrication. Interscience, New York, N.Y., 1962.

Matweb, 1999. Aluminum 6061-T6: 6061-T651. Material Property Data. Blacksburg, 1999. https://www.matweb.com/search/datasheet.aspx?MatGUID=d5ea75577b1b49e8ad03caf007db5ba8.

Ribeiro, A.S., Gölze, M., 2017. Decision rules applied to conformity assessment. European federation of national associations of measurement. Brussels, 2017 Testing anad Analytical Laboratories 14. Technical Report 1/2017. https://eurolab-d.de/files/eurolab_technical_report_no.1-decision_rules_applied_to_conformity_assessment-2017_final.pdf.

Tungsten Carbide Powder – GTP, 2008. Tungsten Carbide Technical Bulletin. Global Tungsten & Powders Corporation. Towanda, PA, USA, 2008. https://www.yumpu.com/en/document/view/35181805/tungsten-carbide-powder-gtp.

UKAS, 2022. United Kingdom accreditation service. Decision rules and statements of conformity. LA (La. Agric.) 48 (4), 47. Middlesex, 2022. https://www.ukas.com/wp-content/uploads/schedule_uploads/759162/LAB-48-Decision-Rules-and-Statements-of-Conformity.pdf.

Weber, C.E., Hirsch, H.H., 1955. Dispersion-type fuel elements. Geneve, Switzerland, August 8-20. In: Proceedings of the International Conference on the Peaceful Uses of Atomic Energy, 1955.Paper No. P/561.